Computers & Structures Vol. 35, No. 4, pp. 505–522, 1990
Printed in Great Britain.

0045-7949/90 $3.00 + 0.00
Pergamon Press plc

PLATE BENDING ELEMENTS WITH DISCRETE CONSTRAINTS: NEW TRIANGULAR ELEMENTS

O. C. Zienkiewicz,† R. L. Taylor,‡ P. Papadopoulos‡ and E. Oñate§

†Institute for Numerical Methods in Engineering, University of Wales, Swansea, U.K.
‡Department of Civil Engineering, University of California at Berkeley, Berkeley, CA 94720, U.S.A.
§E.T.S. Ingenieros de Caminos, Canales, y Puertos, Universidad Politécnica de Cataluña, Barcelona, Spain

Abstract—In recent years a series of elements based on Reissner–Mindlin assumptions and using discrete (collocation type) constraints has been introduced. These elements have proved to be very effective, however their relation to straightforward mixed approximations has not been clear. In this paper this relationship is discussed and the reasons for their success explained. This allows new and effective triangular elements to be developed. The presentation shows the close relationships with the DKT (Discrete Kirchhoff Theory) element previously available only for thin plates and allows extension of their applications.

1. INTRODUCTION

The problem of plate bending was one of the first tackled by the finite element method in the early 1960s and yet today it is still subject to much research, designed to improve the performance of bending elements. The subject is of much importance in structural engineering and satisfactory solutions of plate bending form a necessary prerequisite for the analysis of shells.

The original approaches invariably utilized the thin plate, Kirchhoff theory used in a direct (irreducible) manner and immediately encountered the difficulties of imposing the C^1 continuity of shape functions necessary for the finite element formulation. Later work approached plates directly as an approximation to three dimensional analysis [1, 2], or, which is equivalent, by the use of the Reissner [3]–Mindlin [4], *thick* plate theory. This by-passed the difficulties caused by the C^1 requirement but introduced its own problems immediately. In particular, locking behavior was observed as the thickness was reduced and various artifices had to be used to eliminate such effects. The most successful of these was the introduction of *reduced* or *selective* integration procedures [5–9]. However, even this was not generally sufficient and almost all elements of that type proved non-robust, failing under diverse circumstances. Other approaches have also been proposed, including the use of incompatible modes in the description of the transverse shear strain [10].

The thick plate theory can, of course, be used as a basis for a mixed finite element approximation if shear forces and displacements are approximated independently. Indeed, the realization of this led Malkus and Hughes [6] to demonstrate the equivalence of selective integration with a penalized version of the mixed form. More recently a fuller analysis [11] of the mixed formulation which is, of course, valid for both 'thick' and 'thin' plates indicated why the failure of 'thick' forms occurs frequently in practice. Indeed, this analysis showed how successful elements could be developed and the first fully robust element based on the direct Reissner–Mindlin approach was introduced only very recently [12].

Since 1981, however, a very successful approach to the formulation of elements based on the 'thick' theory was developed using *smoothed shear strain fields* and concentrated, discrete, constraints [13–17]. The relationship of this approach to direct, mixed, approximation was not, however, clear (at least to the present authors) and in particular it was not evident why such elements should be exempt from the various convergence criteria given in [11]. In this paper we shall attempt to (a) present a comprehensive explanation of various mixed and direct approximations, and (b) show how the procedures can be applied to development of new plate elements generally, and to a triangle in particular.

While the proponents of the thick plate, Mindlin–Reissner approach were overcoming the difficulties mentioned above, those approaching the formulation via the Kirchhoff theory successfully avoided the C^1 continuity requirements, by imposing the Kirchhoff constraints in a 'discrete manner' (often referred to as a Discrete Kirchhoff Theory). The concepts were first introduced as early as 1968 [18] by Wempner *et al.*, but the development of successful elements by this procedure has been continuous up to the present date. References [19–28] list some of the salient stages of this story. It is evident that this direction of progress, which we shall term DKT for short, must be related to the full mixed formulation with discrete constraints and we shall discuss this

relationship here. This does indeed prove to be correct and hence a more unified view of the plate problems can now emerge.

Before proceeding with the main topic of the paper we would like to point out to the reader that the fields of applicability of thick and thin plate approximations are by no means always obvious. Very recently Babuska and Scapolla [29] showed how, in an apparently very thin plate (thickness/span equal to 0.01), errors of *ca* 5% in displacements can occur between the true behavior and that predicted on the basis of Kirchhoff hypotheses. For this reason the approaches based *a priori* on thick plate equations, but which are capable of representing thin forms, are optimal. It is with such methods that we are concerned here.

2. THE BACKGROUND THEORY

The *thick*, Reissner–Mindlin, theory of plates introduces two assumptions which are physically plausible when the thickness is small compared to other dimensions.

- The first assumption is that the normals to the mid-surface of the plate before deformation remain straight after deformation (but do not necessarily remain normal to it).
- The second assumption is that the stresses normal to the mid-plane direction (and indeed their effects) remain negligible.

With these assumptions it is possible to describe all displacements in the plate by the knowledge of the rotations and displacements of the mid-plate.

We can thus write

$$u = z\theta_x(x, y)$$
$$v = z\theta_y(x, y)$$
$$w = w(x, y), \tag{1}$$

where θ_x, θ_y and w are dependent only on the two in-plane coordinates x, y (Fig. 1), and z is the direction normal to it.

The strains in the plate, for planes parallel to x, y, are thus given by the following:

$$\epsilon_x = z\frac{\partial\theta_x}{\partial x}$$
$$\epsilon_y = z\frac{\partial\theta_y}{\partial y}$$
$$\gamma_{xy} = z\left[\frac{\partial\theta_x}{\partial y} + \frac{\partial\theta_y}{\partial x}\right] \tag{2}$$

and in the vertical direction

$$\gamma_{xz} = \left[\theta_x + \frac{\partial w}{\partial x}\right]$$
$$\gamma_{yz} = \left[\theta_y + \frac{\partial w}{\partial y}\right]. \tag{3}$$

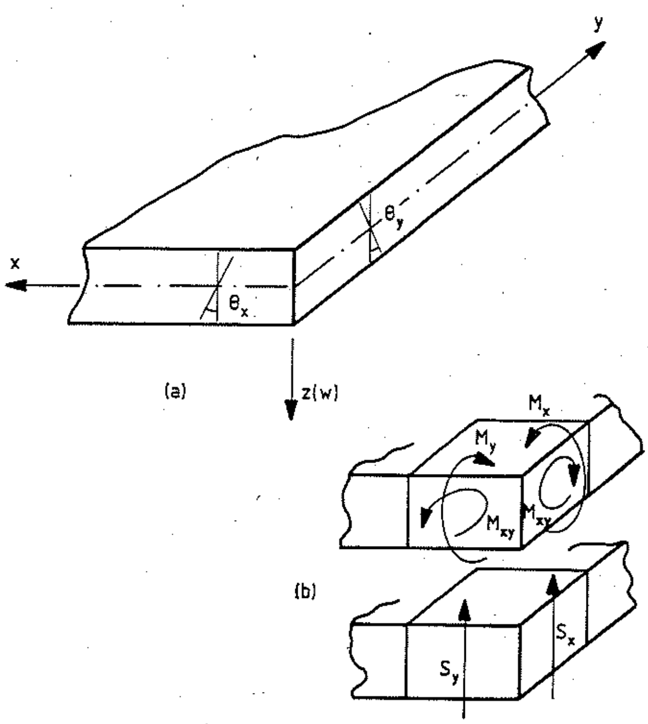

Fig. 1. Definitions of variables for plate equations. (a) Displacements and rotations. (b) Stress resultants.

Constitutive relations allow all stresses and hence stress resultants to be evaluated. For isotropic, homogeneous, elasticity we have for the bending moments defined below

$$M_x = \int_{-t/2}^{t/2} \sigma_x z \, dz$$

$$M_y = \int_{-t/2}^{t/2} \varsigma_y z \, dz$$

$$M_{xy} = \int_{-t/2}^{t/2} \sigma_{xy} z \, dz \tag{4}$$

and the following relations:

$$\mathbf{M} = \mathbf{D}\mathbf{L}\boldsymbol{\theta}; \quad \mathbf{D} = \frac{Et^3}{12(1-\nu^2)} \begin{bmatrix} 1 & \nu & 0 \\ \nu & 1 & 0 \\ 0 & 0 & \dfrac{1-\nu}{2} \end{bmatrix}. \tag{5}$$

Here E and ν are the elastic modulus and Poisson's ratio, t the plate thickness and

$$\mathbf{M}^T = [M_x, M_y, M_{xy}]$$

$$\boldsymbol{\theta}^T = [\theta_x, \theta_y]. \tag{6}$$

The operator $\mathbf{L}$ follows from eqn (2) as

$$\mathbf{L} = \begin{bmatrix} \dfrac{\partial}{\partial x} & 0 \\ 0 & \dfrac{\partial}{\partial y} \\ \dfrac{\partial}{\partial y} & \dfrac{\partial}{\partial x} \end{bmatrix}. \tag{7}$$

Similarly the transverse shear forces are defined by

$$S_x = \int_{-t/2}^{t/2} \tau_{xz} \, dz$$

$$S_y = \int_{-t/2}^{t/2} \tau_{yz} \, dz \tag{8}$$

and the constitutive relation is

$$\mathbf{S} = \alpha[\boldsymbol{\theta} + \nabla w]; \quad \alpha = \kappa G t. \tag{9}$$

Here G is the shear modulus of the material and κ a factor which depends on the plate properties (a commonly used value of κ is 5/6).

Two equilibrium equations need to be added to the above relations. The first relates the bending moments to shear forces and is simply

$$\mathbf{L}^T\mathbf{M} + \mathbf{S} = \mathbf{0}. \tag{10}$$

The second is a statement of lateral equilibrium

$$\nabla^T\mathbf{S} + q = 0. \tag{11}$$

Various possibilities exist regarding the choice of variables to be retained in the final equation system when approximation is to be made. We shall here retain w, $\boldsymbol{\theta}$, and $\mathbf{S}$ and write the system as

$$\mathbf{L}^T\mathbf{D}\mathbf{L}\boldsymbol{\theta} + \mathbf{S} = \mathbf{0}. \tag{12a}$$

From eqn (9),

$$\frac{1}{\alpha}\mathbf{S} - (\boldsymbol{\theta} + \nabla w) = \mathbf{0} \tag{12b}$$

and repeating eqn (11)

$$\nabla^T\mathbf{S} + q = 0. \tag{12c}$$

The equation system forms the basis of a *mixed formulation* if $\boldsymbol{\theta}$, w and $\mathbf{S}$ are approximated independently. The *thin* plate, Kirchhoff approximation is simply a limiting case in which $\alpha = \infty$ and eqn (12b) is then the well-known constraint

$$\boldsymbol{\theta} + \nabla w = \mathbf{0}. \tag{13}$$

This ensures that during deformation the normals remain normal to the middle plane of the plate.

The formulation of eqn (12) is *mixed* as it is possible, by use of eqn (12b), to eliminate one of the variables, $\mathbf{S}$, from the system when an irreducible form is obtained. The latter is indeed the basis from which most thick plate approximations start but as a finite value of α is needed to perform the elimination such forms are not available for the thin plate limit.†

It is generally anticipated, however, that the thin plate behavior will be approximated to as α becomes progressively larger and tends to infinity. However, this is not true in most finite element approximations unless the equivalent mixed form of eqn (12) is solvable. If it is not, singularities and/or locking will occur.

The equation system (12) is frequently interpreted as a minimization of total potential energy defined as [30]

$$\Pi = \frac{1}{2}\int_\Omega (\mathbf{L}\boldsymbol{\theta})^T\mathbf{D}(\mathbf{L}\boldsymbol{\theta}) \, d\Omega + \frac{1}{2}\int_\Omega \mathbf{S}^T\alpha^{-1}\mathbf{S} \, d\Omega - \int \Omega \, wq \, d\Omega \tag{14a}$$

subject to the constraints given by eqn (12b), i.e.

$$\frac{1}{\alpha}\mathbf{S} = (\boldsymbol{\theta} + \nabla w). \tag{14b}$$

This constraint, if directly eliminated at the above level, leads to a standard penalized form which we discussed above; if the constraint is incorporated in

† It is of course possible to eliminate $\mathbf{S}$ and $\boldsymbol{\theta}$ even if α is infinite using appropriate differentiation. This leads to the biharmonic thin plate equations.

a new functional by means of a Lagrangian multiplier we shall find the well known Hellinger–Reissner variational theorem, etc.

Other possibilities exist in the solution as we will show in the next section.

3. THE FINITE ELEMENT APPROXIMATION TO THE MIXED FORM

If we wish to retain a solution capable of covering the full *thick* and *thin* range (i.e. not failing when $\alpha = \infty$), it is necessary to approximate all the variables and write†

$$\boldsymbol{\theta} = \mathbf{N}_\theta \bar{\boldsymbol{\theta}} \quad w = N_w \bar{\mathbf{w}} \quad \mathbf{S} = \mathbf{N}_S \bar{\mathbf{S}}. \tag{15}$$

In the above, $\mathbf{N}_\theta$, $\mathbf{N}_w$ and $\mathbf{N}_s$ stand for the appropriate shape functions in the x, y domain, and $\bar{\boldsymbol{\theta}}$, $\bar{\mathbf{w}}$ and $\bar{\mathbf{S}}$ are the associated (nodal) parameters.

All possible approximations can be obtained using suitable weighting functions [28] on the equation system (12) and the resulting equation will always be of the type

$$\begin{bmatrix} \mathbf{A} & \mathbf{B} & \mathbf{0} \\ \bar{\mathbf{B}}^T & \mathbf{H}/\alpha & \mathbf{C} \\ \mathbf{0} & \bar{\mathbf{C}}^T & \mathbf{0} \end{bmatrix} \begin{Bmatrix} \bar{\boldsymbol{\theta}} \\ \bar{\mathbf{S}} \\ \bar{\mathbf{w}} \end{Bmatrix} = \begin{Bmatrix} \mathbf{f}_1 \\ \mathbf{f}_2 \\ \mathbf{f}_3 \end{Bmatrix}. \tag{16}$$

In the particular case of the approximation arising via the variational principle the above equation will be symmetric, but this is not always necessarily so.

In another paper [11] we have shown that it is necessary, if an algebraic solution of the system of eqn (16) in the limiting case when $\alpha = \infty$ is possible, to satisfy

$$n_\theta + n_w \geqslant n_S \tag{17}$$
$$n_S \geqslant n_w,$$

where n_θ, n_w and n_S stand for the number of variables in each set of parameters $\bar{\boldsymbol{\theta}}$, $\bar{\mathbf{w}}$ and $\bar{\mathbf{S}}$, respectively.

The above inequalities have to be satisfied also for various element patches as a condition which is necessary (although not always sufficient) for convergence [32, 33].

In [11] we have examined a number of currently used elements and found that all failed this stringent test. Indeed only the element of [23] and an element introduced more recently by Arnold and Falk [34] satisfy the above count requirements and indeed converge in all circumstances. In Fig. 2 both these elements are shown in a single element patch test in which displacements on the boundary are either fully constrained (Test C) or relaxed to a minimum restraining only the rigid body modes (Test R). In both cases these tests are satisfactory passed and the reader can verify that the same occurs in larger element assemblies.

4. THE DISCRETE APPROXIMATION ON ELEMENT BOUNDARIES

The elements developed by Bathe and Dvorkin [13, 14] and Hinton and Huang [15, 16] fall into the general category we have just discussed, but use a very special shear resultant interpolation.‡

The first element of this series is a bilinear quadrilateral, or its special form, the bilinear rectangle, illustrated in Fig. 3. Here $\mathbf{S}$ is specified by interpolating S_x and S_y components separately in the manner shown.

If the substitution of the above interpolation is made in a general formulation obtainable from the Hellinger–Reissner variational principle (or indeed using the standard Galerkin weighting approximation) we see immediately that the fully restrained patch test on a single element fails (as indeed does the test on element assemblies).

Now $n_\theta = 0$, $n_S = 4$ and $n_w = 0$, as shown in Fig. 3, noting that the parameters $\bar{\mathbf{S}}$ are not restrained. Indeed, the patch test will fail even more dramatically if an assembly of elements is considered as shown in Fig. 4.

Difficulties can, however, be overcome by the use of *discrete*, collocation-type approximations to eqn (12b). If the equation appropriate to a particular component is satisfied at a single point of the side (by using Dirac delta weighting) we can write for such a point as A placed in the middle of side 1–2 of Fig. 3

$$\frac{1}{\alpha} S_y = \frac{1}{\alpha} \bar{S}_y = \theta_y + \frac{\partial w}{\partial y} = \frac{\bar{\theta}_y^1 + \bar{\theta}_y^2}{2} + \frac{\bar{w}^2 - \bar{w}^1}{h} \tag{18}$$

with three similar equations on the other sides.

This immediately ensures that $\bar{S}_y$ is explicitly determined by the two end values of $\bar{\boldsymbol{\theta}}$ and $\bar{\mathbf{w}}$ and that their prescription uniquely determines $\bar{S}_y$ values. On boundaries these are therefore no longer free parameters to be taken into account in the patch test. Now for the single element test $n_S = 0$ and the patch count is passed.

Indeed the unique specification of $\bar{S}_y$ by the end values means that at element interfaces such as shown in Fig. 4 only a single value of $\bar{S}_y$ (or $\bar{S}_x$) is a free parameter. In that figure it is shown that the patch test, though not yet completely passed, is much more closely approximated.

The idea can, of course, be extended to include more variables as shown by Hinton and Huang [15, 16]. In their element, with bi-quadratic θ and w approximation, each of the shear components

† More general interpolation may be used. For example, we could write $w = \mathbf{N}_w \bar{\mathbf{w}} + \mathbf{N}_{w\theta} \bar{\boldsymbol{\theta}}$ so that displacements for transverse displacements involve parameters of the rotation. This is the form that the thin plate solution uses where the transverse displacement interpolation involves nodal parameters of displacement and rotations (e.g. Hermite interpolations). This type of interpolation also results from application of constraints [31].

‡ In fact, the interpolation is not for the shear resultants but for the quantity $\mathbf{S}/\alpha = \gamma =$ shear strain. Results will, however, still be identical if α is assumed constant.

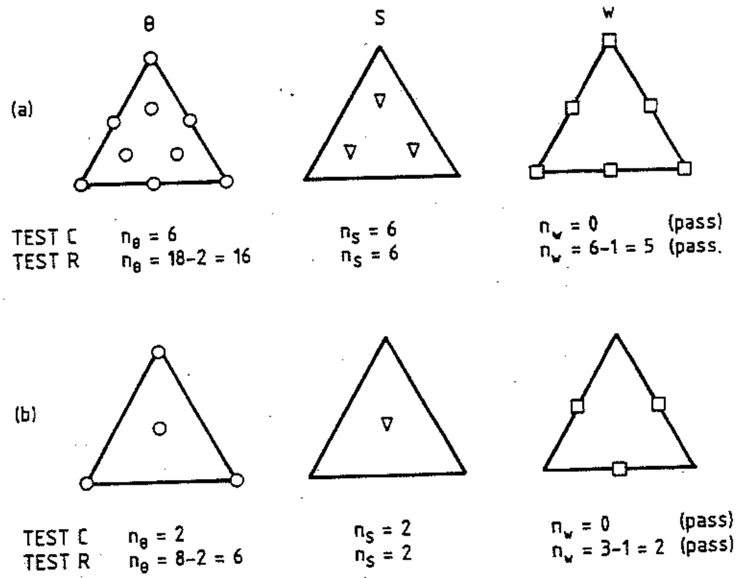

Fig. 2. Single element patch test count. (a) Element of [12] (Zienkiewicz–Lefebvre). (b) Element [34] (Arnold). ○ Node with θ variables (2 DOF). ▽ Node with S variables (2 DOF). □ Node with w variables (1 DOF). TEST C (constrained). All θ–w prescribed on boundary. TEST R (relaxed). 2θ and $1w$ variables prescribed on boundary. Necessary condition: $n_\theta + n_w > n_s$; $n_s > n_w$.

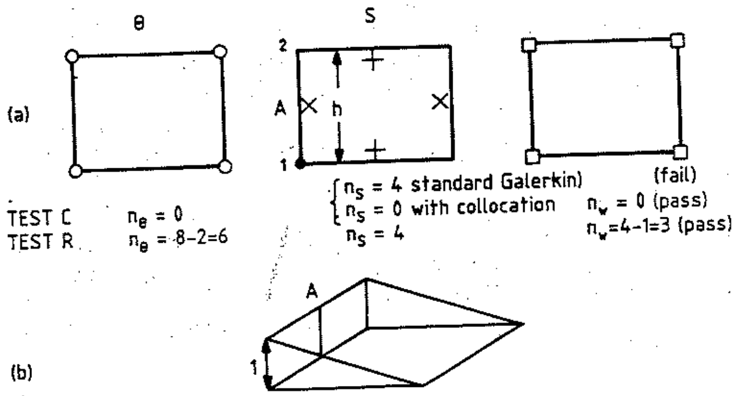

Fig. 3. The Dvorkin–Bathe element. (a) The element parameters: ○ θ nodes (2 DOF); + S_y nodes (1 DOF) (eliminated at element level); × S_x nodes (1 DOF) (eliminated at element level); □ w nodes (1 DOF). (b) Shape function for S_x at node A. Note: with collocation type of constraint along 1–2 S_y at A is determined value by θ/w at (1) and (2) and hence not a full parameter. This ensures that the test is satisfied.

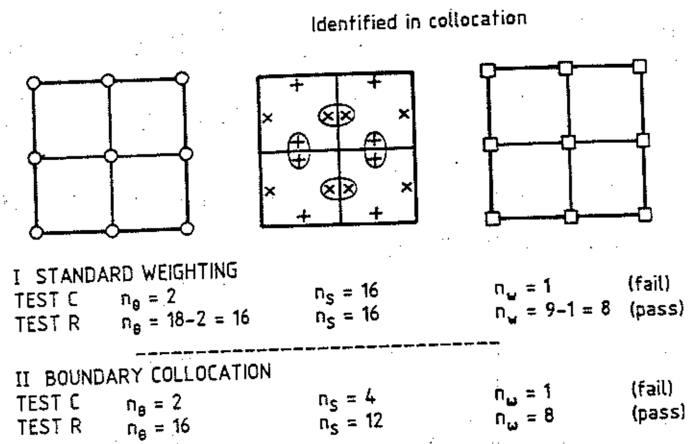

Fig. 4. Four element patch count test on quadrilateral with S_x, S_y interpolation (Dvorkin–Bathe element). I. Standard weighting. II. Collocation on boundary. Note: (1) the Dvorkin–Bathe element fails this test, end is suspect in some circumstances (not robust); (2) with collocation S boundary values are prescribed by displacements on same line.

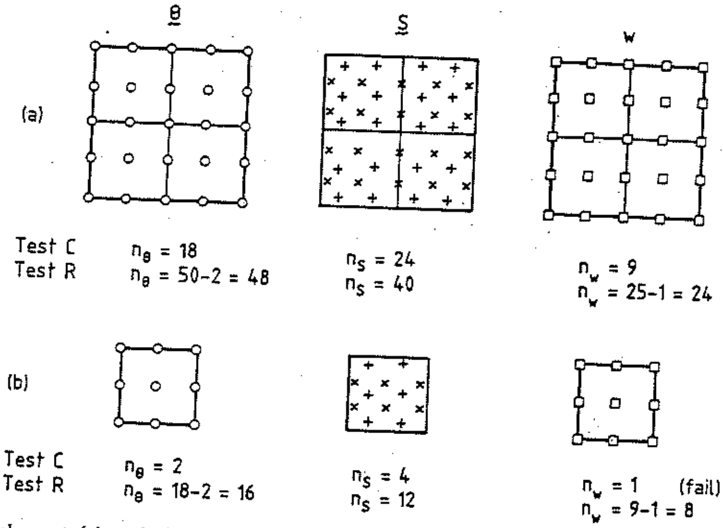

Fig. 5. Four element (a) and single element (b) patch count test on the Hinton–Huang element (two point boundary collocation only shown). Note: this is a robust element as all multiple element patch tests passed.

is interpolated by placing two nodes on the appropriate sides, as shown in Fig. 5. Though additional parameters (and collocation points) are placed in the interior of the element, the parameters on interfaces are uniquely defined by the $\bar{\theta}$ and $\bar{\mathbf{w}}$ lying on those faces and thus are constrained fully on the boundary. This formulation fails the test for a single element but passes the test for multiple assemblies and is more robust than the Bathe–Dvorkin version.

It should be noted that point collocation is not, of course, the only way to ensure the desired effect. Any weighting specified only on the element boundaries will suffice to achieve this. For instance, requiring that in the previous example we have

$$\int_1^2 \left[\frac{1}{\alpha} S_y - \theta_y - \frac{\partial w}{\partial y}\right] \mathrm{d}\Gamma = 0 \tag{19}$$

or indeed specifying collocation points not placed at the center of an element boundary will be satisfactory though not necessarily equally accurate. Results given in Sec. 7 are for a triangular element which has shear constraints expressed in the form of eqn (19).

5. ELEMENT STIFFNESS MATRICES

The discrete constraint equations approximating to eqn (12b) can be written as

$$\frac{1}{\alpha}\bar{\mathbf{S}} = \mathbf{Q}\begin{Bmatrix}\bar{\boldsymbol{\theta}}\\ \bar{\mathbf{w}}\end{Bmatrix} = \mathbf{Q}_\theta\bar{\boldsymbol{\theta}} + \mathbf{Q}_w\bar{\mathbf{w}} \tag{20}$$

providing the number of constraint relationships is equal to that of the number of variables S. Here Q is an easily found matrix and this allows the variables S to be eliminated from eqns (12a) and (12c). These in turn can be discretized by appropriate weighting. However it is difficult *a priori* to determine the weighting which will result in symmetric stiffness matrices and for this reason it is convenient to return to the variational form given by eqns (14a) and (14b).

Now the variational function of eqn (14a) can be written in a discrete form and eqn (20), together with the shear approximations, may be used to eliminate S.

We can thus insert into eqn (14a)†

$$\boldsymbol{\theta} = \mathbf{N}_\theta\bar{\boldsymbol{\theta}}; \quad w = \mathbf{N}_w\bar{\mathbf{w}} \tag{21a}$$

and

$$\mathbf{S} = \mathbf{N}_S\bar{\mathbf{S}} = \alpha\mathbf{N}_S[\mathbf{Q}_\theta\bar{\boldsymbol{\theta}} + \mathbf{Q}_w\bar{\mathbf{w}}] \tag{21b}$$

and minimize appropriately with respect to the parameters $\bar{\boldsymbol{\theta}}$ and $\bar{\mathbf{w}}$.

On insertion of the above into the functional we have immediately

$$\begin{aligned}\Pi = {} & \frac{1}{2}\int_\Omega [\mathbf{L}\mathbf{N}_\theta\bar{\boldsymbol{\theta}}]^T\mathbf{D}[\mathbf{L}\mathbf{N}_\theta\bar{\boldsymbol{\theta}}]\,\mathrm{d}\Omega + \frac{1}{2}\int_\Omega [\mathbf{N}_S\mathbf{Q}_\theta\bar{\boldsymbol{\theta}} \\ & + \mathbf{N}_S\mathbf{Q}_w\bar{\mathbf{w}}]^T\alpha[\mathbf{N}_S\mathbf{Q}_\theta\bar{\boldsymbol{\theta}} + \mathbf{N}_S\mathbf{Q}_w\bar{\mathbf{w}}]\,\mathrm{d}\Omega \\ & - \int_\Omega [\mathbf{N}_w\bar{\mathbf{w}}]^T q\,\mathrm{d}\Omega\end{aligned} \tag{22}$$

and on minimization we obtain

$$\begin{bmatrix}\mathbf{K}_{\theta\theta} & \mathbf{K}_{\theta w}\\ \mathbf{K}_{w\theta} & \mathbf{K}_{ww}\end{bmatrix}\begin{Bmatrix}\bar{\boldsymbol{\theta}}\\ \bar{\mathbf{w}}\end{Bmatrix} = \begin{Bmatrix}\mathbf{f}_1\\ \mathbf{f}_2\end{Bmatrix} \tag{23}$$

† Note that the interpolation for w may need to be generalized if it involves nodal parameters $\bar{\mathbf{w}}$ and $\bar{\boldsymbol{\theta}}$.

with

$$\mathbf{K}_{\theta\theta} = \int_\Omega [(\mathbf{L}\mathbf{N}_\theta)^T \mathbf{D}(\mathbf{L}\mathbf{N}_\theta) + (\mathbf{N}_S \mathbf{Q}_\theta)^T \alpha (\mathbf{N}_S \mathbf{Q}_\theta)] \, \mathrm{d}\Omega \, .$$

$$\mathbf{K}_{\theta w} = \int_\Omega (\mathbf{N}_S \mathbf{Q}_\theta)^T \alpha (\mathbf{N}_S \mathbf{Q}_w) \, \mathrm{d}\Omega = \mathbf{K}_{w\theta}^T$$

$$\mathbf{K}_{ww} = \int_\Omega (\mathbf{N}_S \mathbf{Q}_w)^T \alpha (\mathbf{N}_S \mathbf{Q}_w) \, \mathrm{d}\Omega.$$

6. OBLIQUE COORDINATES

The derivations of the preceding sections have been limited to simple rectangles and a direct interpolation of S_x and S_y shear components. Of course it is easy to generalize to curvilinear shapes using isoparametric or other mapped coordinates and to interpolate S_ξ and S_ζ in a similar way, defining

$$\frac{1}{\alpha} S_\xi = \theta_\xi + \frac{\partial w}{\partial \xi}, \text{ etc.} \tag{24}$$

Parameters defining $\bar{S}_\xi$ on element sides will now be necessary but the general algebra will be identical.† It will, of course, be necessary in the final computation to transfer the components to a Cartesian system, and we omit here the details which are adequately described in [13–16, 18].

7. NEW TRIANGULAR ELEMENTS

The concepts expounded in the previous section allow many new variants of *discretely constrained* elements to be derived. As an example we introduce three new triangles which are subsequently tested by applications to several example problems. Results from the test are given in Sec. 9.

7.1. *Quadratic triangle—six-node element*

We consider first a triangle which is illustrated in Fig. 6. The interpolations for the transverse displacement, w, and rotation fields, $\boldsymbol{\theta}$, are assumed to vary quadratically over the element. Using hierarchical forms for the mid-side parameters the interpolations may be written as

$$\boldsymbol{\theta} = \sum_{i=1}^{3} L_i \bar{\boldsymbol{\theta}}^i + \sum_{i=1}^{3} 4 L_i L_j \Delta\bar{\boldsymbol{\theta}}^k \tag{25}$$

and

$$w = \sum_{i=1}^{3} L_i \bar{w}^i + \sum_{i=1}^{3} 4 L_i L_j \Delta\bar{w}^k, \tag{26}$$

† In the development of triangular elements we introduce tangential components along each edge which we shall refer to as θ_S and S_S.

‡ The function mod(i, j) is equal to $i - (i/j)*j$ where integer arithmetic is used evaluate i/j.

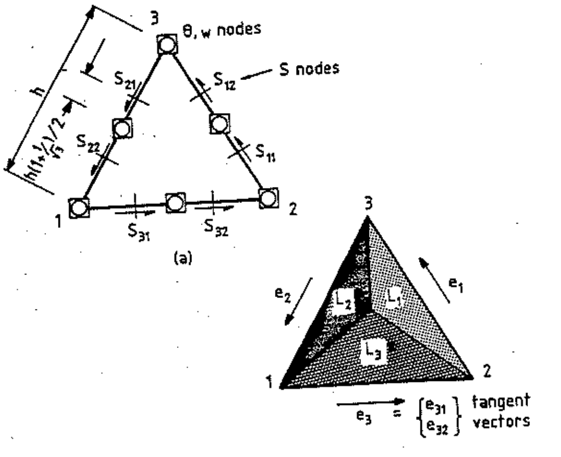

Fig. 6. The new quadratic triangular plate element. (a) The parameters; $\bar{\theta}$—12 DOF; $\bar{\omega}$—6 DOF; S—6 DOF. (b) Area coordinates and notation.

where L_i are the standard area coordinates, and $\Delta\bar{\boldsymbol{\theta}}^k$ and $\Delta\bar{w}^k$ are hierarchical displacement and rotation parameters at the element mid-side‡

$$j = \text{mod}(i, 3) + 1; \quad k = \text{mod}(j, 3) + 1.$$

The interpolation for the transverse shear resultants is less obvious. Here six nodal values of shears parallel to the sides of the triangle and located at Gauss points as shown in Fig. 6a uniquely define a linear distribution of shear resultants. Accordingly, we write first

$$\mathbf{S} = \sum_{i=1}^{3} L_i \bar{\mathbf{S}}^i. \tag{27}$$

The coefficients $\bar{\mathbf{S}}^i$ can be uniquely determined by writing equations at the six constraint points and finally the full interpolation expression defining the shear resultant shape functions becomes

$$\mathbf{S} = \sum_{i=1}^{3} \frac{L_i}{\Delta_i} \begin{bmatrix} e_{ky} & -e_{jy} \\ -e_{kx} & e_{jx} \end{bmatrix} \begin{Bmatrix} g_1 \bar{S}_{j1} + g_2 \bar{S}_{j2} \\ g_2 \bar{S}_{k1} + g_1 \bar{S}_{k2} \end{Bmatrix}, \tag{28}$$

where $\bar{S}_{j1}$ and $\bar{S}_{j1}$ and $\bar{S}_{j2}$ are the tangential shear resultants at the two points on the j-edge,

$$g_1 = \tfrac{1}{2}(1 - \sqrt{3})$$
$$g_2 = \tfrac{1}{2}(1 + \sqrt{3})$$
$$\Delta_i = e_{jx} e_{ky} - e_{jy} e_{kx}.$$

In the above the components of $\mathbf{e}_j$ are the direction cosines of the sides on which $L_j = 0$. Fuller details of the derivation are given in Appendix A. A stiffness matrix for this element is computed using eqn (23) and in the numerical examples section the results are labeled TRI-6.

Table 7. Sensitivity test on a clamped, uniformly loaded plate

(x, y) coordinates of interior node	$w(0, 0)$ $\times 10^{-3}$	% error (relative)
(3.00, 3.00)	3.35729	0.00
(3.25, 3.25)	3.35462	0.08
(3.50, 3.50)	3.34660	0.31
(3.75, 3.75)	3.33313	0.72
(4.00, 4.00)	3.31356	1.30
(4.25, 4.25)	3.28403	2.18
(3.00, 3.25)	3.35548	0.05
(3.00, 3.50)	3.35318	0.12
(3.00, 3.75)	3.35025	0.21
(3.00, 4.00)	3.34640	0.32
(3.00, 4.25)	3.34123	0.48
(3.00, 4.50)	3.33431	0.68
(2.75, 3.25)	3.35606	0.04
(2.50, 3.50)	3.35991	0.08
(2.25, 3.75)	3.37107	0.41
(2.00, 4.00)	3.39206	1.04
(1.75, 4.25)	3.42524	2.02
(1.50, 4.50)	3.47146	3.40

presented may be directly used in standard finite element packages. By suitable choice of constraints the elements generated pass the mixed patch test and, thus, do not lock and are not singular in the thin plate limit. The methodology presented also provides a unification with previous developments which used discrete Kirchhoff constraints.

New triangular elements are presented and shown to give good results on a series of standard test problems. For the limiting case of thin plate behavior, the DRM element (for discrete Reissner–Mindlin element) is shown to be identical to the popular DKT triangle introduced by Dhatt [25]. Unlike the DKT element, however, the DRM element also may be used for analysis of 'thick' plate problems.

Since interpolation is provided for all the variables in the formulation the extension to transient, as well as non-linear applications is straightforward. Furthermore, we believe that the DRM element presented is suitable for use with adaptive mesh refinement schemes.

REFERENCES

1. S. Ahmad, B. M. Irons and O. C. Zienkiewicz, Curved thick shell and membrane elements with particular reference to axisymmetric problems. *Proc. 2nd Conf. on Matrix Methods in Structural Mechanics* (Edited by R. M. Bader *et al.*). Wright-Patterson Air Force Base, Ohio (1968).
2. S. Ahmad, B. M. Irons and O. C. Zienkiewicz, Analysis of thick and thin shell structures by curved finite elements. *Int. J. Numer. Meth. Engng* **2**, 419–451 (1970).
3. E. Reissner, The effect of transverse shear deformation on the bending of elastic plates. *J. appl. Mech.* **12**, 69–76 (1945).
4. R. D. Mindlin, Influence of rotatory inertia and shear in flexural motions of isotropic elastic plates. *J. appl. Mech.* **18**, 31–38 (1951).
5. T. J. R. Hughes, R. L. Taylor and W. Kanoknukulchai, A simple and efficient element for plate bending. *Int. J. Numer. Meth. Engng* **11**, 1529–1543 (1977).
6. D. S. Malkus and T. J. R. Hughes, Mixed finite element methods—reduced and selective integration techniques: a unification of concepts. *Comput. Meth. appl. Mech. Engng* **15**, 63–81 (1978).
7. S. F. Pawsey and R. W. Clough, Improved numerical integration of thick slab finite elements. *Int. J. Numer. Meth. Engng* **3**, 575–586 (1971).
8. E. D. L. Pugh, E. Hinton and O. C. Zienkiewicz, A study of quadrilateral plate bending elements with reduced integration. *Int. J. Numer. Meth. Engng* **12**, 1059–1079 (1978).
9. O. C. Zienkiewicz, J. Too and R. L. Taylor, Reduced integration technique in general analysis of plates and shells. *Int. J. Numer. Meth. Engng* **3**, 275–290 (1971).
10. J. C. Nagtegaal, S. Nakazawa and M. Tateishi, On the construction of optimal Mindlin type plate and shell elements. In *Finite Element Methods for Plate and Shell Structures, Volume 1: Element Technology* (Edited by T. J. R. Hughes and E. Hinton), pp. 348–364. Pineridge Press, Swansea (1986).
11. O. C. Zienkiewicz and D. Lefebvre, Three field mixed approximation and the plate bending problem. *Commun. appl. Numer. Meth.* **3**, 301–309 (1987).
12. O. C. Zienkiewicz and D. Lefebvre, A robust triangular plate bending element of the Reissner–Mindlin type. *Int. J. Numer. Meth. Engng* **26**, 1169–1184 (1988).
13. K. J. Bathe and E. N. Dvorkin, A four node plate bending element based on Mindlin/Reissner plate theory and mixed interpolation. *Int. J. Numer. Meth. Engng* **21**, 367–383 (1985).
14. E. N. Dvorkin and K. J. Bathe, A continuum mechanics based four node shell element for general non-linear analysis. *Engng Comput.* **1**, 77–88 (1984).
15. E. Hinton and H. C. Huang, A family of quadrilateral Mindlin plate elements with substitute shear strain fields. *Comput. Struct.* **23**, 409–431 (1986).
16. H. C. Huang and E. Hinton, A nine node Lagrangian Mindlin element with enhanced shear interpolation. *Engng Comput.* **1**, 369–380 (1984).
17. T. J. R. Hughes and T. E. Tezduyar, Finite elements based upon Mindlin plate theory with particular reference to the four node bilinear isoparametric element. *J. appl. Mech.* **46**, 587–596 (1981).
18. G. A. Wempner, J. T. Oden and D. K. Dross, Finite element analysis of thin shells. *Proc. Am. Soc. civ. Engrs* **EM6**, 1273–94 (1968).
19. J. T. Baldwin, A. Razzaque and B. M. Irons, Shape function subroutine for an isoparametric thin plate element. *Int. J. Numer. Meth. Engng* **7**, 431–440 (1973).
20. J. L. Batoz, An explicit formulation for an efficient triangular plate bending element. *Int. J. Numer. Meth. Engng* **18**, 1077–1089 (1982).
21. J. L. Batoz, K. J. Bathe and L. W. Ho, A study of three node triangular plate bending elements. *Int. J. Numer. Meth. Engng* **15**, 1771–1812 (1980).
22. J. L. Batoz and M. Ben Tohar, Evaluation of a new quadrilateral thin plate bending element. *Int. J. Numer. Meth. Engng* **18**, 1655–1677 (1982).
23. K. J. Bathe, E. N. Dvorkin and L. W. Ho, On discrete Kirchhoff and isoparametric shell elements for non-linear analysis—an assessment. *Comput. Struct.* **16**, 89–98 (1983).
24. M. A. Crisfield, A four-noded thin-plate bending element using shear constraints—a modified version of Lyon's element. *Comput. Meth. appl. Mech. Engng* **38**, 93–120 (1983).
25. G. S. Dhatt, Numerical analysis of thin shells by curved triangular elements based on discrete Kirchhoff hypothesis. In *Proc. Symp Appl. of F.E.M. in Civil Engng* (Edited by W. R. Rowan and R. M. Hackett), pp. 255–278. Vanderbilt University, Nashville, TN (1969).

S. S. Murthy and R. H. Gallagher, A triangular thin-shell finite element based on discrete Kirchhoff theory. *Comput. Meth. appl. Mech. Engng* **54,** 197–222 (1986).

H. Stolarski and M. Y. M. Chiang, Thin plate elements with relaxed Kirchhoff constraints. *Int. J. Numer. Meth. Engng* **26,** 913–934 (1988).

O. C. Zienkiewicz, *The Finite Element Method*, 3rd Edn. McGraw–Hill, London (1977).

I. Babuska and T. Scapolla, Benchmark computation and performance evaluation for a rhombic plate bending problem. *Int. J. Numer. Meth. Engng* **27,** 155–179 (1989).

K. Washizu, *Variational Methods in Elasticity and Plasticity*. Pergamon, Oxford (1948).

A. Tessler and S. B. Dong, On a hierarchy of conforming Timoshenko beam elements. *Comput. Struct.* **14,** 335–344 (1981).

32. R. L. Taylor, O. C. Zienkiewicz, J. C. Simo and A. H. C. Chan, The patch test—a condition for assessing FEM convergence. *Int. J. Numer. Meth. Engng* **22,** 32–62 (1986).

33. O. C. Zienkiewicz, S. Qu, R. L. Taylor and S. Nakazawa, The patch test for mixed formulations. *Int. J. Numer. Meth. Engng* **23,** 1873–1883 (1986).

34. D. N. Arnold and R. S. Falk, A uniformly accurate finite element method for Mindlin–Reissner plate. IMA Preprint Series No. 307, Institute for Mathematics and its Applications, University of Minnesota, April 1987.

35. L. P. R. Lyons, A general finite element system with special analysis of cellular structures. Doctoral dissertation, Imperial College of Science and Technology, London (1977).

36. A. Razzaque, Finite element analysis of plates and shells. Doctoral dissertation, Civil Engineering, University College of Swansea (1972).

37. A. Razzaque, Program for triangular bending elements with derivative smoothing. *Int. J. Numer. Meth. Engng* **6,** 333–345 (1973).

38. B. M. Irons, The semiloof shell element. In *Finite Elements for Thin Shells and Curved Members* (Edited by D. G. Ashwell and R. H. Gallagher), Ch. 11, pp. 197–222. John Wiley, New York (1976).

39. S. Timoshenko and S. Woinowsky-Krieger, *Theory of Plates and Shells*. McGraw–Hill, New York (1959).

40. R. W. Clough and J. L. Tocher, Finite element stiffness matrices for analysis of plates in bending. *Proc. Conf. on Matrix Meth. in Struct. Mech.* (Edited by R. M. Bader *et al.*), pp. 515–545. AFFDL-TR-66-80, WPAFB, OH (1966).

41. T. J. R. Hughes, *The Finite Element Method.* Prentice–Hall, Englewood Cliffs, NJ (1987).

42. L. S. D. Morley, *Skew Plates and Structures*, International Series of Monographs in Aeronautics and Astronautics. Macmillan, New York (1963).

43. J. C. Simo, D. D. Fox and M. S. Rifai, On a stress resultant geometrically exact shell model. Part II: the linear theory; computational aspects. *Comput. Meth. appl. Mech. Engng* **73,** 53–92 (1989).

APPENDIX A: TRANSVERSE SHEAR RESULTANT INTERPOLATION

The interpolation described in Sec. 7 for the transverse shear resultant is given by

$$\mathbf{S} = \sum_{i=1}^{3} L_i \bar{\mathbf{S}}^i. \tag{A1}$$

The $\bar{\mathbf{S}}^i$ are to be determined by satisfying discrete edge constraints for the tangential shear resultant [32]. The tangential shear resultant on side k of the triangle (i.e. the side where $L_k = 0$) is

$$S_k = \mathbf{e}_k \cdot \mathbf{S}, \tag{A2}$$

where

$$\mathbf{e}_k = [e_{kx}, e_{ky}] = [\cos\omega_k, \sin\omega_k], \tag{A3}$$

and ω_k is the angle that the tangent makes with the x-axis (see Appendix B).

Equation (A2) is used at two points on each side of the triangle to define six independent values of tangential shear resultant. The two points on each edge are picked to correspond to the two-point Gauss values, which on the interval 0 to 1 (range of each area coordinate) are given by

$$p_1 = \frac{1}{2}\left(1 + \frac{1}{\sqrt{3}}\right), \quad p_2 = \frac{1}{2}\left(1 - \frac{1}{\sqrt{3}}\right). \tag{A4}$$

Accordingly

$$\bar{S}_{k1} = S_k(L_{i1}, L_{j1}, L_{k1}) = \mathbf{e}_k \cdot \mathbf{S}(L_{i1}, L_{j1}, L_{k1}), \tag{A5a}$$

where

$$L_{i1} = p_1, \quad L_{j1} = p_2, \quad L_{k1} = 0.$$

Similarly, for the second point

$$\bar{S}_{k2} = S_k(L_{i2}, L_{j2}, L_{k2}) = \mathbf{S}(L_{i2}, L_{j2}, L_{k2}) \cdot \mathbf{e}_k \tag{A5b}$$

with

$$L_{i2} = p_2, \quad L_{j2} = p_1, \quad L_{k2} = 0.$$

In the above the i, j, k sequence is given by (see Fig. 6) $j = \mathrm{mod}(i, 3) + 1$, $k = \mathrm{mod}(j, 3) + 1$.

Evaluation of eqns (A5a) and (A5b) on each edge using eqn (A1) gives

$$\bar{S}_{k1} = \mathbf{e}_k \cdot (p_1 \bar{\mathbf{S}}^i + p_2 \bar{\mathbf{S}}^j). \tag{A6a}$$

Similarly, for the second point

$$\bar{S}_{k2} = \mathbf{e}_k \cdot (p_2 \bar{\mathbf{S}}^i + p_1 \bar{\mathbf{S}}^j). \tag{A6b}$$

Adding and subtracting eqns (A6a) and (A6b) and simplifying the results we obtain

$$\mathbf{e}_k \cdot \bar{\mathbf{S}}^i = g_1 \bar{S}_{k1} + g_2 \bar{S}_{k2} \tag{A7a}$$

and

$$\mathbf{e}_k \cdot \bar{\mathbf{S}}^j = g_2 \bar{S}_{k1} + g_1 \bar{S}_{k2}, \tag{A7b}$$

where

$$g_1 = \tfrac{1}{2}(1 + \sqrt{3})$$
$$g_2 = \tfrac{1}{2}(1 - \sqrt{3}). \tag{A8}$$

The parameters $\bar{\mathbf{S}}^i$ now may be expressed in terms of the $\bar{S}_{i1}$ and $\bar{S}_{i2}$ using eqn (A7a) directly, permuting the subscripts on eqn (A7b) to correspond to the i value, and writing the pair of equations

$$\begin{Bmatrix} \mathbf{e}_k \cdot \bar{\mathbf{S}}^i \\ \mathbf{e}_j \cdot \bar{\mathbf{S}}^i \end{Bmatrix} = \begin{Bmatrix} g_1 \bar{S}_{k1} + g_2 \bar{S}_{k2} \\ g_2 \bar{S}_{j1} + g_1 \bar{S}_{j2} \end{Bmatrix}. \tag{A9}$$

Upon noting that

$$\begin{Bmatrix} \mathbf{e}_k \cdot \bar{\mathbf{S}}^i \\ \mathbf{e}_j \cdot \bar{\mathbf{S}}^i \end{Bmatrix} = \begin{bmatrix} e_{kx} & e_{ky} \\ e_{jx} & e_{jy} \end{bmatrix} \begin{Bmatrix} \bar{S}^i_x \\ \bar{S}^i_y \end{Bmatrix}. \tag{A10}$$

the solution is given by

$$\begin{Bmatrix} \bar{S}^i_x \\ \bar{S}^i_y \end{Bmatrix} = \frac{1}{\Delta_i}\begin{bmatrix} e_{jy} & -e_{ky} \\ -e_{jx} & e_{kx} \end{bmatrix}\begin{Bmatrix} g_1\bar{S}_{k1} + g_s\bar{S}_{k2} \\ g_2\bar{S}_{j1} + g_1\bar{S}_{j2} \end{Bmatrix}, \tag{A11}$$

where

$$\Delta_i = e_{kx}e_{jy} - e_{ky}e_{jx}.$$

Substitution of eqn (A11) into eqn (A1) gives the result presented as eqn (31) of Sec. 7.

For the case in which the tangential shear is to be constant on each edge we may note that setting

$$\bar{S}_{k0} = \bar{S}_{k1} = \bar{S}_{k2} \tag{A12}$$

results immediately in the results given in eqn (32).

APPENDIX B: CONSTRAINT EQUATIONS FOR $\bar{S}_{kn}$

The parameters $\bar{S}_{k1}$, etc. may be expressed in terms of the nodal values of the transverse displacement, $\bar{\mathbf{w}}$, and the rotations, $\bar{\boldsymbol{\theta}}$, using results in eqn (24) specialized for the tangential direction. Accordingly,

$$\frac{1}{\alpha}\bar{S}_{k1} = \left(\frac{\partial w}{\partial t} + \theta_t\right)\bigg|_1 = \pm\frac{\bar{w}^j - \bar{w}^i + 4(3^{-1/2})\Delta\bar{w}^k}{h_k} + \frac{1}{2}\mathbf{e}_k\cdot[\bar{\boldsymbol{\theta}}^i + \bar{\boldsymbol{\theta}}^j + 3^{-1/2}(\bar{\boldsymbol{\theta}}^i - \bar{\boldsymbol{\theta}}^j)] + \frac{2}{3}\Delta\theta^k. \tag{B1a}$$

Similarly, for the second point

$$\frac{1}{\alpha}\bar{S}_{k2} = \left(\frac{\partial w}{\partial t} + \theta_t\right)\bigg|_2 = \pm\frac{\bar{w}^j - \bar{w}^i - 4(3^{-1/2})\Delta\bar{w}^k}{h_k} + \frac{1}{2}\mathbf{e}_k\cdot[\bar{\boldsymbol{\theta}}^i + \bar{\boldsymbol{\theta}}^j - 3^{-1/2}(\bar{\boldsymbol{\theta}}^i - \bar{\boldsymbol{\theta}}^j)] + \frac{2}{3}\Delta\theta^k, \tag{B1b}$$

where h_k is the length of the k-side of the element.

The parameter $\bar{S}_{k0}$ for the DRM element may be deduced using eqn (24) in eqn (19). After integration along each boundary the result is

$$\frac{1}{\alpha}\bar{S}_{k0} = \int_{\Gamma_k}\left(\frac{\partial w}{\partial t} + \theta_t\right)\mathrm{d}t = \pm\frac{\bar{w}^j - \bar{w}^i}{h_k} + \frac{1}{2}\mathbf{e}_k\cdot(\bar{\boldsymbol{\theta}}^i + \bar{\boldsymbol{\theta}}^j) + \frac{2}{3}\Delta\theta^k. \tag{B2}$$

The $\pm$ ambiguity in eqns (B1) and (B2) is due to the fact that the direction of the tangential shear must be defined by a unique direction on each edge of contiguous elements. Failure to achieve this results in an inconsistent definition of the edge incremental rotation degree of freedom, $\Delta\theta^k$. One way to overcome this difficulty is to define the direction for $\mathbf{e}_k$ in the direction of increasing (global) node numbers for the end points of each element edge, thus establishing a unique value for ω_k. The sign in eqns (B1) and (B2) is chosen to be positive if the direction of $\mathbf{e}_k$ corresponds to that for constructing the boundary integrals, otherwise a negative sign is inserted.

The construction of $\mathbf{Q}_w$ and $\mathbf{Q}_\theta$ in eqn (21b) is obtained by a systematic use of eqn (B1) or (B2) and noting that the shape functions for shear are given by the area coordinates, L_i, as shown in eqn (A1).

The result for a DKT element can be obtained by setting eqn (B2) to zero and expressing each $\Delta\theta^k$ in terms of the nodal parameters at each vertex of the triangle. The resulting element has nine degrees of freedom (three at each node) and is identical to the results given in [20, 21, 25].